Received December 1996
Accepted February 1997

Dual boundary element analysis for cracked bars under torsion

J.T. Chen, K.H. Chen and W. Yeih
Department of Harbor and River Engineering, Taiwan Ocean University, Keelung, Taiwan, and
N.C. Shieh
Department of Mechanical Engineering, Central University, Taiwan

Introduction

In studying the torsion problem using numerical techniques, the analyst may encounter problems with singularities. Singular behavior is often ignored in the expectation that the error will be limited to the vicinity of the singularity. However, it is very important to show how strong the singular behavior is, e.g. the stress intensity factor of fracture mechanics. In finite elements, special singular or hybrid elements are sometimes used instead of the quarter-point rule; MSC/NASTRAN Version 68[1] provides the capabilities of singular CRAC3D and CRAC2D elements for crack problems, but the Laplace equation with singularity has not been developed to the author's knowledge. For problems with a degenerate boundary, e.g. crack problems[2-7], flow around sheet piles[8,9] and thin airfoil in aerodynamics[10,11], singularity exists, and the dual integral formulation has been applied successfully. Using the dual integral formulation, all the well-posed boundary value problems can be solved even though a degenerate boundary is present. It is well known that dual boundary element (DBEM) is particularly suitable for the problem of extreme localization and concentration with singularity. The DBEM solution is based on the complete formulation of the dual integral equations. The long standing abstruseness of the nonunique problem in BEM has been solved, and the general purpose program of boundary element potential 2-D (BEPO2D) has been implemented[11].

In this paper, the dual BEM is extended to solve a problem of a cracked bar under torsion. The condition number versus the finite thickness of the crack will show the ill-conditioned behavior using conventional BEM. Numerical experiments for solution instability due to ill-posedness will be shown. For the sake of computational efficiency, the area integral formula for torsion rigidity will be transformed into two boundary integrals. Finally, several examples will be solved using two software packages, the BEPO2D and SDRC-IDEAS programs using DBEM and FEM, respectively. The results will be compared with analytical solutions to access their accuracy. Also, the torsion rigidities for cracks with different lengths and orientations will be discussed.

Engineering Computations, Vol. 15 No. 6, 1998, pp. 732-749,

Formulation for torsion problems of a cracked bar

The problem of a cracked bar under torsion can be formulated as a Poisson equation as follows[12,13]:

$$\nabla^2 \Psi(x,y) = -2, \qquad (x,y) \in D, \tag{1}$$

where Ψ is the torsion (Prandtl) function, ∇^2 is the Laplacian operator and D is the domain. The boundary condition is

$$\Psi(x,y) = 0, \qquad (x,y) \text{ on the boundary } B = S + C^+ + C^-, \tag{2}$$

where S is the normal boundary, and C^+ and C^- are the crack boundaries as shown in Figure 1. Since equation (1) contains the body source term, the problem can be reformulated as

$$\nabla^2 \Psi^*(x,y) = 0, \qquad (x,y) \in D \tag{3}$$

and the boundary condition is changed to

$$\Psi^*(x,y) = (x^2 + y^2)/2, \qquad (x,y) \text{ on the boundary } B \tag{4}$$

Where

$$\Psi^* = \Psi + \tilde{\Psi} \text{ and } \tilde{\Psi} = (x^2 + y^2)/2.$$

This new problem of equation (3) can be used to find the solution for a Laplace equation with Dirichelet data in equation (4), which is very easy to implement using DBEM (e.g. the BEPO2D program is used in this study).

The torsion function Ψ can be obtained from Ψ^* by superimposing $\tilde{\Psi}$, and the torque can then be determined by

$$M_z = \iint_A (x\tau_{yz} - y\tau_{xz})dxdy, \tag{5}$$

where τ_{yz} and τ_{xz} are the shearing stress determined by $\tau_{yz} = -\alpha G \frac{\partial \Psi}{\partial x}$ and $\tau_{xz} = \alpha G \frac{\partial \Psi}{\partial y}$, A is the area of the cross section, G is the shear modulus and α denotes the twist angle per unit length.

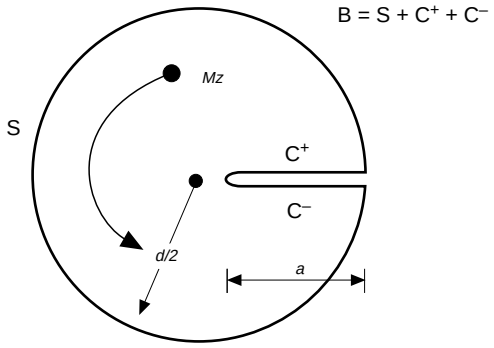

Figure 1.
A cracked torsion bar under torsion

By employing the Green's second identity and equation (1), the area integral in equation (5) can be transformed into a boundary integral and an area integral as follows:

$$\begin{aligned} M_z &= \iint_A (x\tau_{yz} - y\tau_{xz})dxdy \\ &= -\alpha G \iint_A (x\frac{\partial \Psi}{\partial x} + y\frac{\partial \Psi}{\partial y})dxdy \\ &= -\alpha G \iint_A (\nabla \tilde{\Psi} \cdot \nabla \Psi)dxdy \\ &= -\alpha G \iint_A \nabla \cdot (\tilde{\Psi} \nabla \Psi)dxdy + \alpha G \iint_A \tilde{\Psi} \nabla^2 \Psi dxdy \\ &= -\alpha G \oint_B \tilde{\Psi} \frac{\partial \Psi}{\partial n} dB - \alpha G \iint_A (x^2 + y^2)dxdy. \end{aligned} \tag{6}$$

The induced area integral of the second term on the right hand side of the equal sign in equation (6) can be reformulated into a boundary integral again by using the Gauss theorem as follows:

$$\begin{aligned} -\alpha G \iint_A (x^2 + y^2)dxdy &= \frac{-\alpha G}{16} \iint_A \nabla^2 \{(x^2 + y^2)^2\}dxdy \\ &= \frac{-\alpha G}{16} \oint_B \frac{\partial \{(x^2 + y^2)^2\}}{\partial n} dB. \end{aligned} \tag{7}$$

Dual boundary element analysis for a cracked bar

The torsion problem can be simulated by using the mathematical model of the Laplace equation as shown in equation (3). Now, we will consider the boundary integral formulation for numerical analyses. For the classical Laplace problem in Figure 1, the equations may be generally described as follows:

Governing equation:

$$\nabla^2 \Psi^*(x) = 0\,,\ x\ in\ D. \tag{8}$$

Boundary conditions:

$$\Psi^*(s) = f(s),\ s\ on\ B_1 \tag{9}$$

$$\frac{\partial \Psi^*(s)}{\partial n_s} = g(s),\ s\ on\ B_2, \tag{10}$$

where $f(s)$ and $g(s)$ denote the known boundary data, B_1 and B_2 are the boundaries and n_s is the normal vector on the boundary point s. In the torsion

problem of equations (3) and (4), no Neumann boundary condition on B_2 is present.

Using the Green's identity, the first equation of the dual regular boundary integral equations for the domain point x can be derived as follows:

$$2\pi\Psi^*(x) = \int_B T(s,x)\Psi^*(s)dB(s) - \int_B U(s,x)\frac{\partial\Psi^*(s)}{\partial n_s}dB(s), \tag{11}$$

where

$$U(s,x) = ln(r) \tag{12}$$

$$T(s,x) = \frac{\partial U(s,x)}{\partial n_s}, \tag{13}$$

in which r is the distance between the field point x and the source point s. After taking the normal derivative of equation (11), the second equation of the dual regular boundary integral equations for the domain point x can be derived:

$$2\pi\frac{\partial\Psi^*(x)}{\partial n_x} = \int_B M(s,x)\Psi^*(s)dB(s) - \int_B L(s,x)\frac{\partial\Psi^*(s)}{\partial n_s}dB(s), \tag{14}$$

where

$$L(s,x) = \frac{\partial U(s,x)}{\partial n_x} \tag{15}$$

$$M(s,x) = \frac{\partial^2 U(s,x)}{\partial n_x \partial n_s}, \tag{16}$$

in which n_x is the normal vector for the field point x. Equations (11) and (14) are termed dual regular boundary integral equations for the domain point x. The explicit form of the kernel functions can be found in[11]. By tracing the field point x to the boundary, the dual singular boundary integral equations for the boundary point x can be derived:

$$\pi\Psi^*(x) = C.P.V.\int_B T(s,x)\Psi^*(s)dB(s) - R.P.V.\int_B U(s,x)\frac{\partial\Psi^*(s)}{\partial n_s}dB(s) \tag{17}$$

$$\pi\frac{\partial\Psi^*(x)}{\partial n_x} = H.P.V.\int_B M(s,x)\Psi^*(s)dB(s) - C.P.V.\int_B L(s,x)\frac{\partial\Psi^*(s)}{\partial n_s}dB(s), \tag{18}$$

where *R.P.V.*, *C.P.V.* and *H.P.V.* denote the Riemann principal value, Cauchy principal value and Hadamard or Mangler principal value, respectively.

Equations (17) and (18) are called dual singular boundary integral equations for the boundary point x. It must be noted that equation (18) can be derived just by applying the operator of the normal derivative to equation (17). Differentiation of the Cauchy principal value should be carried out carefully using Leibnitz' rule, and then the finite part can be obtained. The finite part has been termed the Hadamard principal value in fracture mechanics[2] or Mangler's principal value in aerodynamics[14]. The commutative property provides us with two alternatives to calculate the Hadamard principal value analytically[2].

The boundary B contains two parts, the normal boundary S and degenerate boundary, $C^+ + C^-$, as shown in Figure 1 and equation (3).

For $x \in S$, equations (17) and (18) can be rewritten as

$$\pi\Psi^*(x) - C.P.V.\int_S T(s,x)\Psi^*(s)dB(s) - R.P.V.\int_S U(s,x)\frac{\partial\Psi^*(s)}{\partial n_s}dB(s) - \int_{C^-} T(s,x)\Delta\Psi^*(s)dB(s) - \int_{C^+} U(s,x)\Sigma\frac{\partial\Psi^*(s)}{\partial n_s}dB(s) \tag{19}$$

$$\pi\frac{\partial\Psi^*(x)}{\partial n_x} = H.P.V.\int_S M(s,x)\Psi^*(s)dB(s) - C.P.V.\int_S L(s,x)\frac{\partial\Psi^*(s)}{\partial n_s}dB(s) + \int_{C^+} M(s,x)\Delta\Psi^*(s)dB(s) - \int_{C^+} L(s,x)\Sigma\frac{\partial\Psi^*(s)}{\partial n_s}dB(s). \tag{20}$$

For $x \in C+$, the equations can be expressed as

$$\frac{\pi}{2}(\Sigma\Psi^*(x) + \Delta\Psi^*(x)) = C.P.V.\int_{C^+} T(s,x)\Delta\Psi^*(s)dB(s) - R.P.V.\int_{C^-} U(s,x)\Sigma\frac{\partial\Psi^*(s)}{\partial n_s}dB(s) + \int_S T(s,x)\Psi^*(s)dB(s) - \int_S U(s,x)\frac{\partial\Psi^*(s)}{\partial n_s}dB(s) \tag{21}$$

$$\frac{\pi}{2}(\Sigma\frac{\partial\Psi^*(x)}{\partial n_x} + \Delta\frac{\partial\Psi^*(x)}{\partial n_x}) = H.P.V.\int_{C^+} M(s,x)\Delta\phi(s)dB(s) - C.P.V.\int_{C^+} L(s,x)\Sigma\frac{\partial\phi(s)}{\partial n_s}dB(s) + \int_S M(s,x)\Psi^*(s)dB(s) \quad \int_S L(s,x)\frac{\partial\Psi^*(s)}{\partial n_s}dB(s), \tag{22}$$

where the sum and difference for the boundary data on C are defined by

$$\Sigma\Psi^*(s) = \Psi^*(s^+) + \Psi^*(s^-) \tag{23}$$

$$\Delta\Psi^*(s) = \Psi^*(s^+) - \Psi^*(s^-) \tag{24}$$

$$\Sigma\frac{\partial\Psi^*}{\partial n}(s) = \frac{\partial\Psi^*}{\partial n}(s^+) + \frac{\partial\Psi^*}{\partial n}(s^-) \tag{25}$$

$$\Delta\frac{\partial\Psi^*}{\partial n}(s) = \frac{\partial\Psi^*}{\partial n}(s^+) - \frac{\partial\Psi^*}{\partial n}(s^-). \tag{26}$$

Equations (23) to (26) tell us that the number of unknowns on the degenerate boundary doubles; therefore, the additional hypersingular integral equation of equation (22) is necessary. The dual boundary integral equations for the boundary point provide the complete constraints of all the boundary data for the well-posed boundary value problem. It must be noted that the compatible relations of boundary data are dependent no matter whether x is on C^+ or on C^- in equations (21) and (22), respectively. Equation (21) has the same equation for x on C^+ or C^-, but equation (22) equations with different signs which are also linearly dependent on each other for x on C^+ and C^-. Nevertheless, equations (21) and (22) for x on C^+ or C^- are linearly independent for the unknowns on the two sides of the degenerate boundary. Hence, equation (22) plays the most important role in a problem with a degenerate boundary.

Dual boundary element discretization and the closed-form integral formulae for the kernel functions

After deriving the above compatible relationships of the boundary data in equations (17) and (18), the boundary integral equations can be discretized by using constant elements, and the resulting algebraic system can be obtained as

$$[\bar{T}_{ij}]\{\Psi^*\}_j = [U_{ij}]\{\frac{\partial \Psi^*}{\partial n}\}_j \tag{27}$$

$$[M_{ij}]\{\Psi^*\}_j = [\bar{L}_{ij}]\{\frac{\partial \Psi^*}{\partial n}\}_j, \tag{28}$$

where [ ] denotes a square matrix, { } a column vector and the elements of the square matrices are

$$U_{ij} = R.P.V. \int U(s_j, x_i) dB(s_j) \tag{29}$$

$$\bar{T}_{ij} = -\pi\delta_{ij} + C.P.V. \int T(s_j, x_i) dB(s_j) \tag{30}$$

$$\bar{L}_{ij} = \pi\delta_{ij} + C.P.V. \int L(s_j, x_i) dB(s_j) \tag{31}$$

$$M_{ij} = H.P.V. \int M(s_j, x_i) dB(s_j). \tag{32}$$

All the above formulae can be integrated analytically; the quadrature rule is used to check the regular integral only. The closed-form solutions of equations (29) to (32) are summarized below.

First, the components of the normal vectors, $\mathbf{n}(x)$ and $\mathbf{n}(s)$, are defined in the following form, respectively:

$$n_1(s) = sin(\theta)\,,\ n_2(s) = -cos(\theta) \tag{33}$$

$$\bar{n}_1(x) = sin(\phi)\,,\ \bar{n}_2(x) = -cos(\phi), \tag{34}$$

where θ and ø are shown in Figure 2(a). Then, the inner and cross products are

$$\mathbf{n}(x) \cdot \mathbf{n}(s) = cos(\phi - \theta) = cos(\phi)cos(\theta) + sin(\phi)sin(\theta) = n_2\bar{n}_2 + n_1\bar{n}_1 \tag{35}$$

$$\mathbf{n}(s) \times \mathbf{n}(x) \cdot \mathbf{e}_k = sin(\phi - \theta) = sin(\phi)cos(\theta) - cos(\phi)sin(\theta) = -\bar{n}_1 n_2 + \bar{n}_2 n_1. \tag{36}$$

using the following transformation as shown in Figure 2(b), we have

$$\left\{ \begin{array}{c} x_r \\ y_r \end{array} \right\} = \left[\begin{array}{cc} cos(\theta) & sin(\theta) \\ -sin(\theta) & cos(\theta) \end{array} \right] \left\{ \begin{array}{c} x_1 - s_1 \\ x_2 - s_2 \end{array} \right\}. \tag{37}$$

For the regular element, the integral formulae is

$$U_{ij} = v\,log\sqrt{v^2 + y_r^2} - v + y_r\,tan^{-1}(v/y_r)\,\Big|_{v=-0.5L_j - x_r}^{v=0.5L_j - x_r} \tag{38}$$

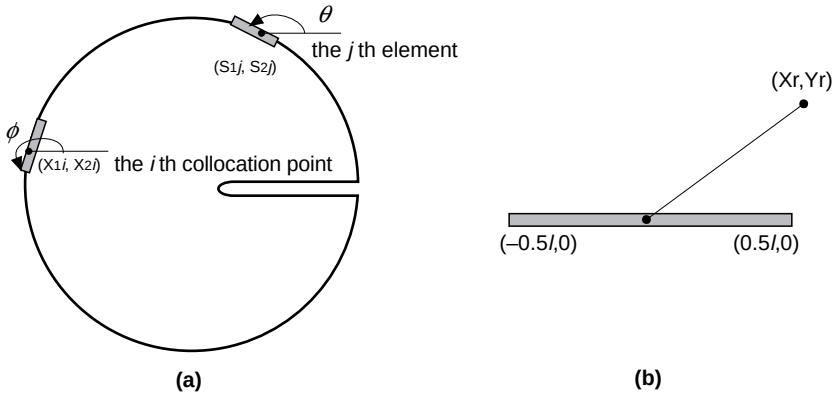

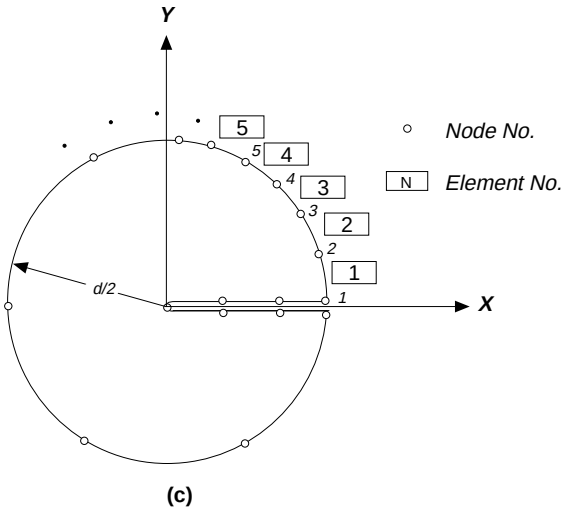

Figure 2.
(a) boundary element discretization
(b) coordinate transformation
(c) boundary element mesh

$$T_{ij} = tan^{-1}(v/y_r) \mid_{v=-0.5L_j-x_r}^{v=0.5L_j-x_r} \tag{39}$$

$$L_{ij} = -cos(\phi-\theta)tan^{-1}(v/y_r) - 0.5\,sin(\phi-\theta)log(v^2+y_r^2) \mid_{v=-0.5L_j-x_r}^{v=0.5L_j-x_r} \tag{40}$$

$$M_{ij} = cos(\phi-\theta)[\frac{tan^{-1}(v/y_r)}{y_r} + \frac{v}{v^2+y_r^2}]$$

$$-y_r\,sin(\phi-\theta)\frac{1}{v^2+y_r^2} - cos(\phi-\theta)\frac{tan^{-1}(v/y_r)}{y_r} \mid_{v=-0.5L_j-x_r}^{v=0.5L_j-x_r}, \tag{41}$$

where L_j is the length of the jth element.

In calculating the above limiting values $x_r \to 0$, $y_r \to 0$) for the singular element, the l'Hospital rule and inverse triangular relations should be considered as follows:

$$tan^{-1}(x) + tan^{-1}(1/x) = \pi/2 \tag{42}$$

$$\lim_{x\to 0}\frac{x}{tan^{-1}(x)} = 1. \tag{43}$$

The closed-form integration for the singular element has the tangent and normal properties of the classical potential theory by way of the $sin(\text{ø} - \theta)$ and $cos(\text{ø} - \theta)$ behavior in equation (41).

To determine the torsion rigidity using equation (6), the following boundary integral can be integrated analytically as follows:

$$\oint_B \tilde{\Psi}\frac{\partial\Psi}{\partial n}dB = \oint_B \tilde{\Psi}\frac{\partial\Psi^*}{\partial n}dB - \oint_B \tilde{\Psi}\frac{\partial\tilde{\Psi}}{\partial n}dB = \sum_{j=1}^{N_t} D_j(\frac{\partial\Psi^*}{\partial n})_j - \sum_{j=1}^{N_t} F_j, \tag{44}$$

where N_t is the total number of boundary elements, $(\frac{\partial\Psi^*}{\partial N})_j$ is the normal gradient of Ψ^* for the jth element, and

$$D_j = \oint_{B_j} \tilde{\Psi}dB = \frac{1}{24}L_j^3 + \frac{1}{2}(s_{1j}^2 + s_{2j}^2)L_j \tag{45}$$

$$F_j = D_j(s_{1j}sin(\theta) - s_{2j}cos(\theta)), \tag{46}$$

in which (s_{1j}, s_{2j}) is the center coordinate of the jth element and B_j is the boundary of the jth element.

To find the contribution of the contour integral around the the crack tip as shown in Figure 3, we have

$$\lim_{\epsilon\to 0}\{-\alpha G\int_0^{\pi}\frac{1}{2}(\epsilon/2)^2\frac{1}{\sqrt{\epsilon/2}}\epsilon d\theta\} = \lim_{\epsilon\to 0}\{-\frac{\alpha}{2}G\pi(\epsilon/2)^{5/2}\} = 0 \tag{47}$$

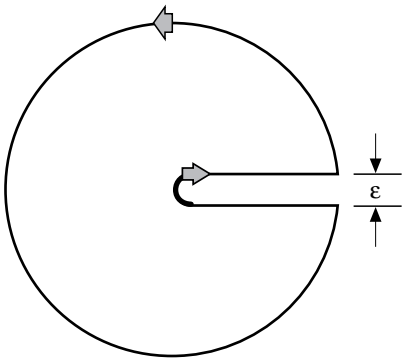

Figure 3.
Contour integration around the crack tip

after using the order of $\frac{\partial \Psi}{\partial n}$ approaching $\frac{1}{\sqrt{\varepsilon/2}}$ near the crack tip.

Another boundary integral in equation (7) can be integrated as follows:

$$\oint_B \frac{\partial\{(x^2+y^2)^2\}}{\partial n} dB = \sum_{j=1}^{N_t} E_j, \tag{48}$$

where

$$E_j = 8D_j(s_{1j}sin(\theta) - s_{2j}cos(\theta)). \tag{49}$$

According to equations (46) and (49), the integrals along the crack surfaces vanish automatically; i.e. the variation of the torsion rigidity due to a crack is only influenced by D_j.

Ill-posedness and its regularization for modeling the degenerate boundary using BEM

To simulate the zero-thickness crack for the bar, a limiting process with a finite thickness, ε, is often employed if a convergent solution can be obtained. In this section, it will be proved that this concept fails using the conventional BEM (UT or LM only) numerically. Figures 4 and 5 show the influence of ε on the torsion function along $y = 0$ for the torsion problem by using the conventional BEM, UT and LM methods, respectively. As ε approaches 0^+, the torsion function in the interior points along the crack does not converge to the exact solution. This numerical error occurs even when the boundary point spacing is very small ($\varepsilon \to 0$). This could easily lead the analyst to believe that he is approaching the correct solution even when his answers actually contain a large error. The cause of the error in the preceding solution is the ill-conditioning of the coefficient matrix instead of the singularity of the crack tip. The ill-conditioned behavior depends on the thickness of the crack as shown in Figure 6 using UT only, LM only or dual methods. It is found that the condition number of dual BEM is less than that of the two methods, UT and LM, respectively. As the thickness

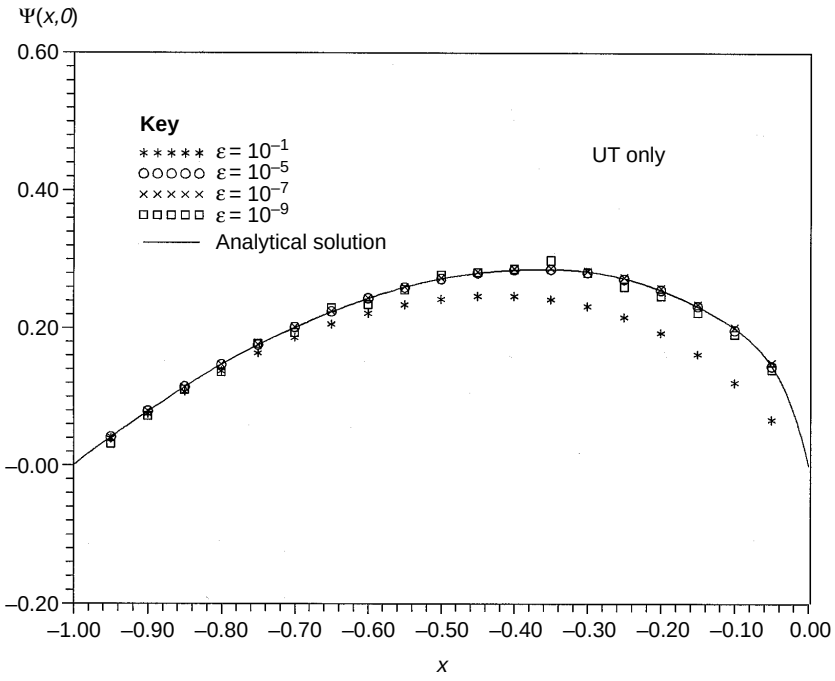

Figure 4.
UT method of solution for the torsion function by means of a limiting process of ε = 0.1, 0.01, 0.001 for the crack thickness

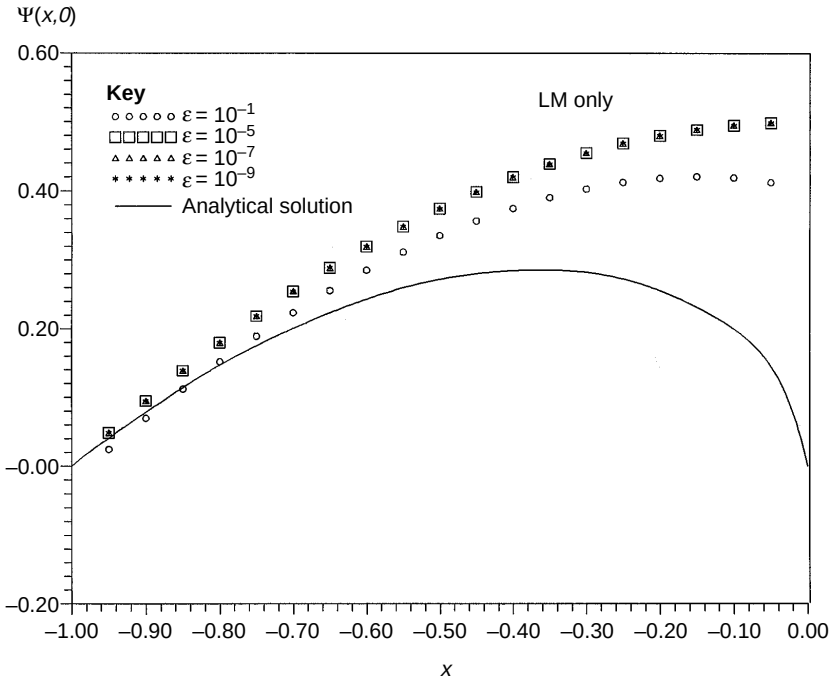

Figure 5.
LM method of solution for the torsion function by means of a limiting process of ε = 0.1, 0.01, 0.001 for the crack thickness

becomes zero, the algebraic equation leads to a singular matrix using UT or LM only. The difficulty with an infinitely thin crack has been solved by dividing the region into two separate zones, the so-called multi-zone method[15-17]. The drawback of the multi-zone method is obvious in that the introduction of artificial boundaries is arbitrary, nonunique, and thus not qualified as an automatic scheme. Also, it results in a larger system of equations than is needed. Instead of employing the multi-zone method, dual BEM can be applied to avoid the ill-conditioned problem as shown in Figure 6. If the thickness of the crack approaches zero but does not equal zero, the order of dependence for the constraint equations by collocating the boundary points on the two sides of the crack is high using the UT or LM methods. To obtain more independent equations on the two sides of the crack boundary, dual BEM must be considered; i.e. one is the UT equation for one side of the crack boundary, and the other is the LM equation for the other side of the crack boundary. When the thickness of the crack is exactly zero, the method combining the UT and LM equations is called dual BEM. Also, dual BEM can be applied to solve the problem when the finite thickness is near zero. Since the constraint equations obtained by collocating the points on the normal boundary have two choices, the UT or LM equations as shown in Figures 7(a) and 8(a), the two results are satisfactory as shown in Figures 7(b) and 8(b), respectively.

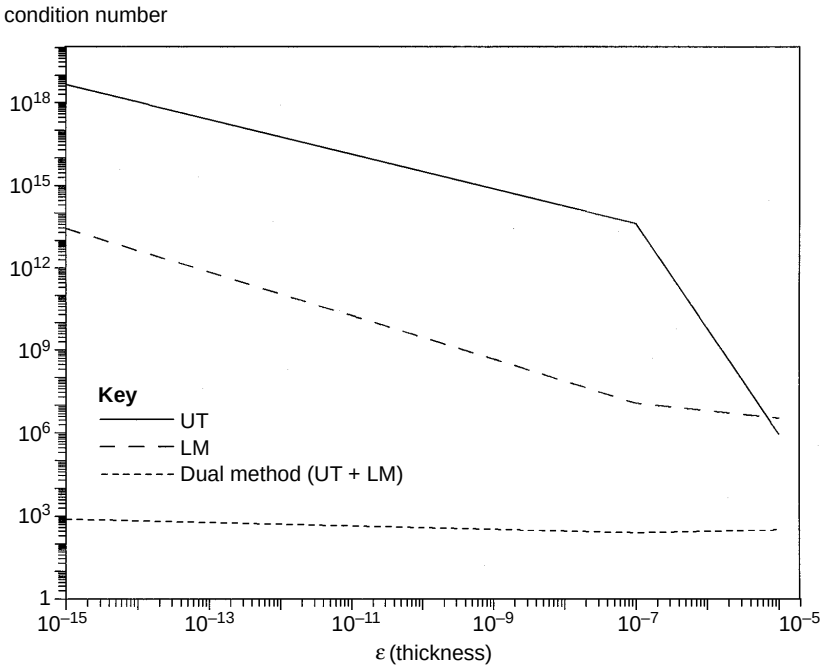

Figure 6.
Condition number using the UT, LM and dual BEM (UT combined LM) methods for different crack thicknesses of ε = 0.1, 0.01, 0.001

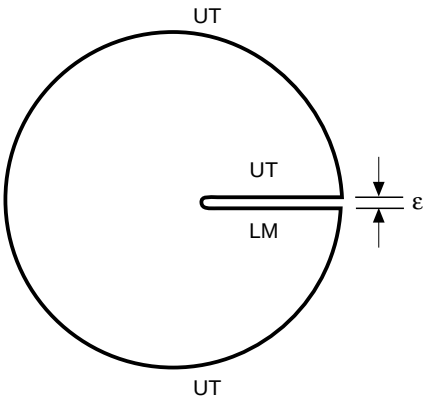

(a)

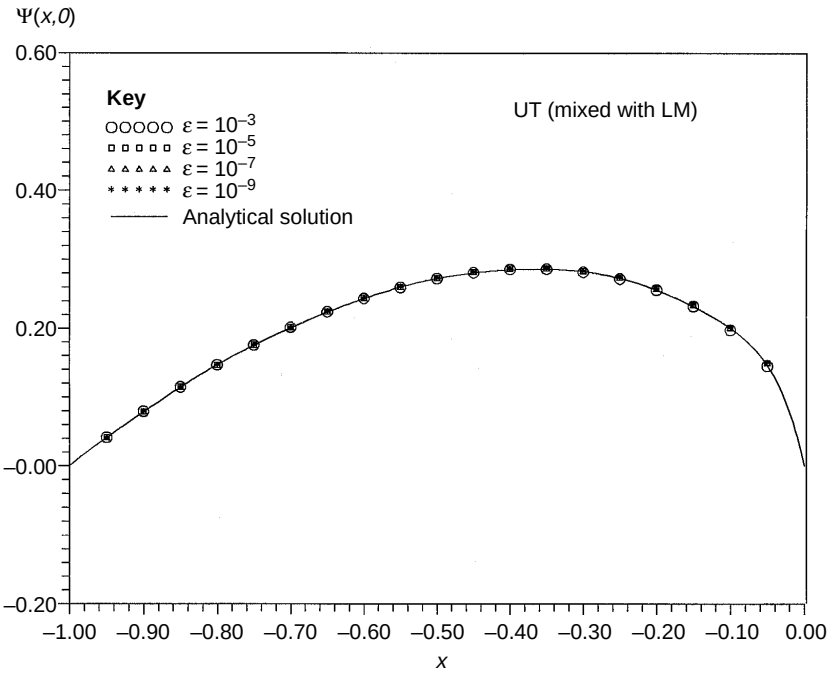

(b)

Figure 7.
(a) constraint equations obtained, (b) dual BEM solution by UT method (mixed with LM method)

Results and discussion of analytical and numerical solutions

The analytical solutions for the torsion rigidities of different length direct cracks are shown below[18]:

(1) For the case of $\frac{a}{d} = 0.50$, where a is the crack length and d is the diameter of the torsion bar, we have the torsion function in polar coordinate $(r, ø)$ and torsion rigidity (M_z) as shown below:

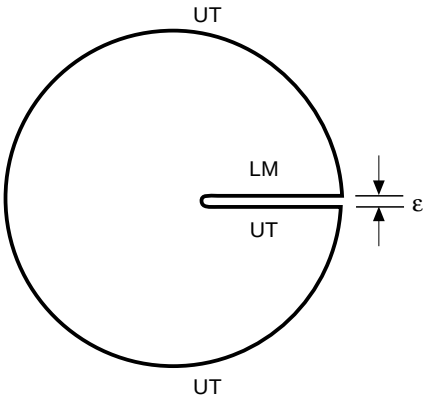

(a)

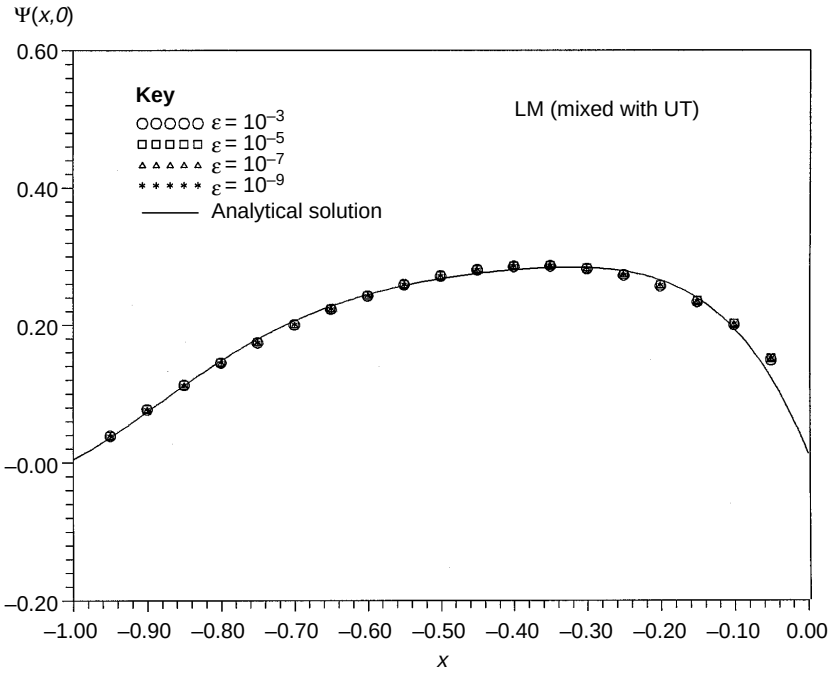

(b)

Figure 8.
(a) constraint equations obtained, (b) dual BEM solution by LM method (mixed with UT method)

$$\Psi(r,\phi) = 32\frac{a^2}{\pi}\sum_{n=0}^{\infty}\frac{(\frac{r}{a})^{(2n+1)/2} - (\frac{r}{a})^2}{(2n+1)[16-(2n+1)^2]}sin\frac{(2n+1)\phi}{2} \tag{50}$$

$$M_z = Ga^4\{\frac{512}{\pi}\sum_{n=0}^{\infty}\frac{1}{(2n+1)^2(2n+5)[16-(2n+1)^2]} - \frac{\pi}{2}\} = 0.878Ga^4. \tag{51}$$

(2) For the case of $\frac{a}{d}$ = 0.25, the torsion function in bipolar coordinate (α, β) can be expressed as

$$u(\alpha,\beta) = a^2 sinh^2\alpha_0\{-\frac{sin^2\beta}{(\cosh\alpha+\cos\beta)^2}\frac{1}{\pi}\sum_{n=0}^{\infty} a_n e^{-(n+\frac{1}{2})(\alpha-\alpha_0)}\sin(n+\frac{1}{2})\beta\}, \quad (52)$$

where

$$a_n = \int_0^{2\pi} \frac{\sin^2\beta\sin(n+\frac{1}{2})\beta}{(\cosh\alpha_0+\cos\beta)^2}d\beta \quad (53)$$

$$\sinh\alpha_0 = \frac{a(d-a)}{d(\frac{1}{2}d-a)}, \qquad (a<\frac{d}{2}). \quad (54)$$

The torsion rigidity (M_z) is obtained as

$$M_z = Ga^4\sinh^4\alpha_0[\frac{2}{\pi}\sinh\alpha_0\sum_{n=0}^{\infty}a_n b_n - \frac{1}{2\pi}\sum_{n=0}^{\infty}(2n+1)a_n^2 - \frac{\pi}{2\sinh^4\alpha_0}], \quad (55)$$

where

$$b_n = \int_0^{2\pi}\frac{\sin^2\beta\sin(n+\frac{1}{2})\beta}{(\cosh\alpha+\cos\beta)^3}d\beta. \quad (56)$$

After some lengthy calculations, we have

$$M_z = 1.28Ga^4.$$

(3) For the case of no crack, $\frac{a}{d}$ = 0, we have the torsion function in the (x,y) coordinate as shown:

$$\Psi(x,y) = \frac{1}{2}(x^2+y^2-\frac{d^2}{4}).$$

The torsion rigidity is found to be

$$M_z = \frac{\pi}{32}Gd^4\theta.$$

For the case of $\frac{a}{d}$ = 0.5, the values of the torsion function along x = 0 and y = 0 are those shown in Figures 9(a) and 9(b), respectively. It is found that the results of dual BEM agree with those of the analytical solution[18] and conventional BEM[13]. According to the two boundary integrals in equations (6) and (7) for torsional rigidity, the nondimensional torsional rigidity is that shown in Figure 10 for a radial crack with different lengths. It is found that the

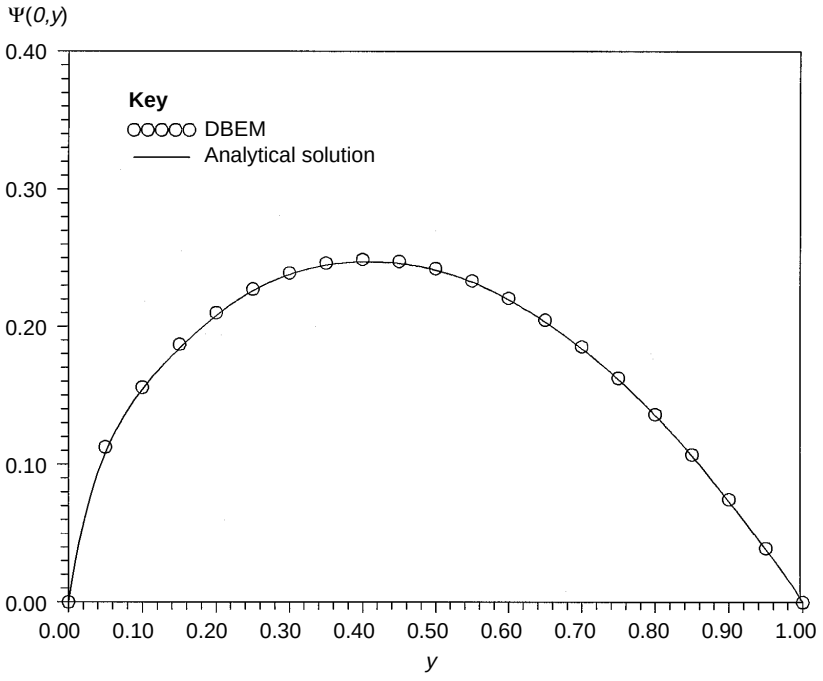

(b)

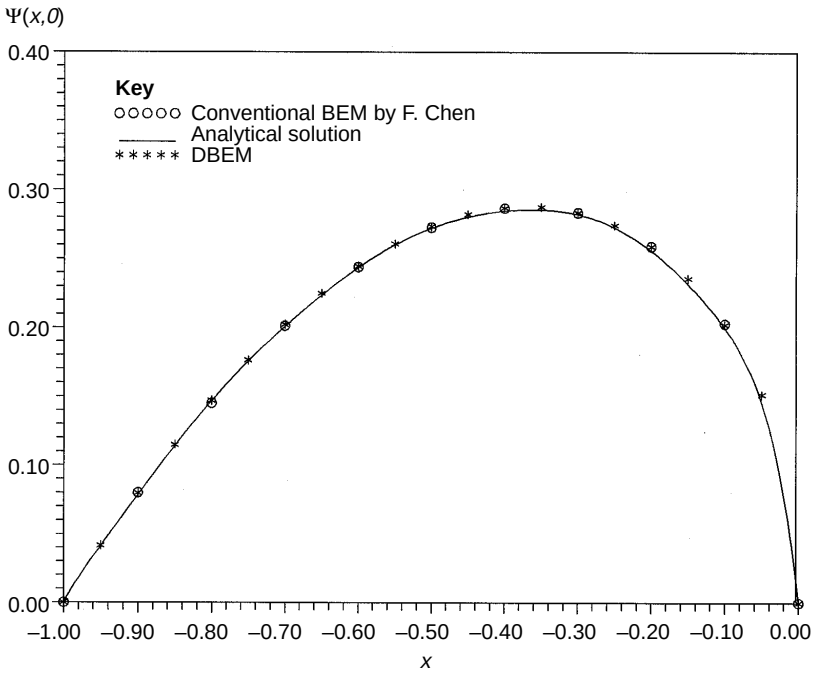

(b)

Figure 9.
(a) airy stress function along $x = 0$, (b) airy stress function along $y = 0$

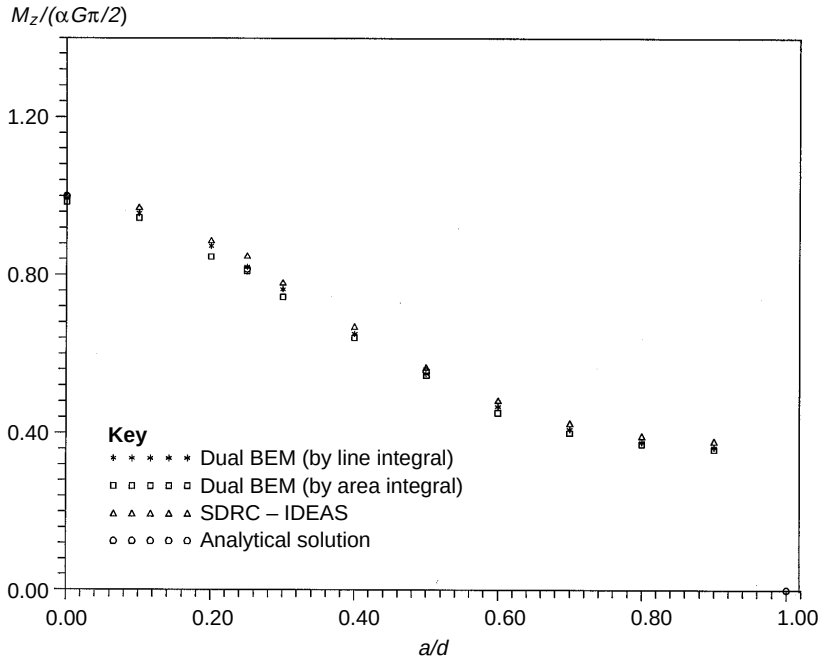

Figure 10.
Torsion rigidities for cracks of different lengths

torsion rigidities for $\frac{a}{d}$ = 0, 0.25 and 0.5 match the analytical solutions in[18]. Also, the results of dual BEM are better than the FEM solutions using the SDRC-IDEAS software.

Similarly, by changing the orientations of the crack angle θ as shown in Figure 11(a), we can construct the curve for M_z versus θ (0° ~ 45°) for a slant crack as shown in Figure 11(b). Although no analytical solutions can be used for comparison, the DBEM results agree well with the FEM solutions.

Conclusions

The dual boundary element method has been applied to solve the torsion problems for a cracked bar. The results show that DBEM provides high solution accuracy and greatly simplifies the modeling. DBEM involves modeling only on the boundary without introducing the artificial boundary as the multi-zone method proposes even though the thickness of the crack is zero. Also, the area integral for torsion rigidity is transformed into two boundary integrals by using the Green's second identity and Gauss theorem; therefore, the domain cell does not need to be discretized. The results have been compared with analytical and FEM solutions, and found to be in good agreement.

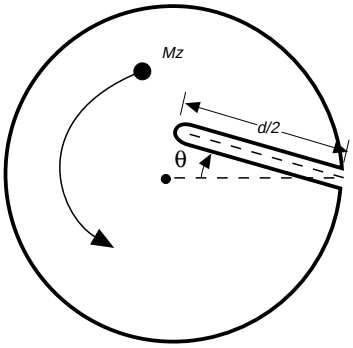

(a)

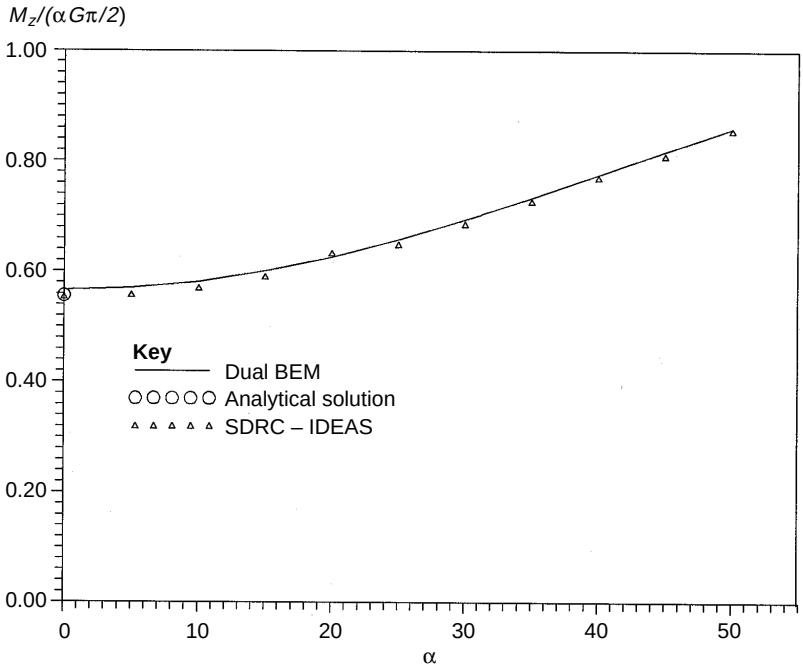

(b)

Figure 11.
(a) torsion bar with a slant crack, (b) torsion rigidities for different angles of crack orientation

References

1. Chen, J.T. *et al., Finite Element Analysis and Engineering Applications Using MSC/NASTRAN,* Northern Gate Publ., Taipei, 1996.
2. Hong, H.-K. and Chen, J.T., "Derivation of integral equations in elasticity", *J. Eng. Mech. Div., ASCE,* Vol. 114 No. 6, Em5, 1988, pp. 1028-44.
3. Chen, J.T., "On Hadamard principal value and boundary integral formulation of fracture mechanics", Master Thesis, Institute of Applied Mechanics, National Taiwan University, 1986.

4. Portela, A., Aliabadi, M.H. and Rooke, D.P., "The dual boundary element method: effective implementation for crack problems", *Int. J. Num. Meth. Engng.,* Vol. 33, 1992, pp. 1269-87.
5. Mi., Y. and Aliabadi, M.H., "Dual boundary element method for three dimensional fracture mechanics analysis", *Engineering Analysis with Boundary Elements,* Vol. 10 No. 2, 1992, pp. 161-71.
6. Fedelinski, P. and Aliabadi, M.H. "The dual boundary element method: J-integral for dynamic stress intensity factors", *Int. J. Fracture,* Vol. 65 No. 4, 1994, pp. 369-81.
7. Leitao, V., Aliabadi, M.H. and Rooke, D.P. "The dual boundary element formulation for elastoplastic fracture mechanics", *Int. J. Num. Meth. in Engng,* Vol. 38, 1995, pp. 315-33.
8. Chen, J.T. and Hong H.-K., "On the dual integral representation of boundary value problem in Laplace equation", *Boundary Elements Abstracts,* Vol. 4 No. 3, 1993, pp. 114-16.
9. Chen, J.T., Hong, H.-K. and Chyuan, S.W., "Boundary element analysis and design in seepage flow problems with sheetpiles", *Finite Elements in Analysis and Design,* Vol. 17, 1994, pp. 1-20.
10. Wang, C.S., Chu, S. and Chen, J.T., "Boundary element method for predicting store airloads during its carriage and separation procedures", in Grilli, S., Brebbia, C.A. and Cheng, A.H.D. (Eds), *Computational Engineering with Boundary Elements, Vol. 1 Fluid and Potential Problems,* 1990, pp. 305-17.
11. Chen, J.T. and Hong, H.-K., *Boundary Element Method,* 2nd Ed., New World Press, Taipei, Taiwan, 1992 (in Chinese).
12. Reismann, H. and Pawlik, P. S., *Elasticity – Theory and Applications,* Wiley, New York, NY, 1980.
13. Chen, F., "Solution of torsion problems by BEM", in Brebbia, C.A. and Rencis, J.J. (Eds), *Boundary Elements XV, Vol. 1, Fluid Flow and Computational Aspects*, CMP, Southampton, 1993, pp. 15-23.
14. Mangler, K.W., "Improper integrals in theoretical aerodynamics", RAE Report, No. 2424, London, 1951.
15. Chang, O.V., "Boundary elements applied to seepage problems in zoned anisotropic soils", MSc. Thesis, Southampton University, 1979.
16. Lafe, O.E., Montes, J.S., Cheng, A.H.D., Liggett, J.A. and Liu, P.L-F., "Singularity in Darcy flow through porous media", *J. Hydra. Div., ASCE* , Vol. 106, HY6, 1980, pp. 977-97.
17. Blandford, G.E., Ingraffea, A.R. and Liggett, J.A., "Two dimensional stress intensity factor computations using the boundary element method", *Int. J. Num. Meth. Engng,* Vol. 17, 1981, pp. 387-404.
18. Lebedev, N.N., Skalskaya, I.P. and Ulfyans, Y.S., *Worked Problems in Applied Mathematics,* translated by Silverman, R.A. Dover, New York, 1965, pp. 185-92.